

國立臺灣大學工學院暨醫學院醫學工程學研究所

碩士論文

Institute of Biomedical Engineering

College of Medicine and College of Engineering

National Taiwan University

Master Thesis



應用於幽門桿菌根除治療之奈米藥物載體開發

The development of nanoparticles for Helicobacter pylori
eradication therapy

黃仲歡

Chung-Huan Huang

指導教授：謝銘鈞 教授

Advisor: Ming-Jium Shieh, M.D., Ph.D.

中華民國 107 年 7 月

July, 2018

國立臺灣大學碩士學位論文
口試委員會審定書

應用於幽門桿菌根除治療之奈米藥物載體開發
The Development Of Nanoparticles For Helicobacter Pylori
Eradication therapy

本論文係黃仲歡君（學號 R05548038）在國立臺灣大學醫學工程
學研究所完成之碩士學位論文，於民國 107 年 7 月 17 日承下列考試
委員審查通過及口試及格，特此證明

口試委員：

謝銘鈞

羅彩月 (指導教授)

林文禮

楊智欽

駱仔云

所長：

黃義侑

致謝



碩班 2 年時間，特別感謝我的指導教授謝銘鈞教授及台大醫院內科部的楊智欽醫師對我的指導和幫助。研究期間的實驗上，非常感謝淑娟學姊 2 年的指導和幫助，謝謝議傑學長教我很多關於菌株培養和分生的實驗、銘賢學長教導我實驗室的各種儀器使用還有平時的聊天和嘴砲。謝謝永遠 18 歲的心怡解決我們行政上面的各種問題、銘峰學長的半夜陪聊和平常神來一筆的各種嘴，還要謝謝欣瑜學姊平常提出很多自己的經驗幫助我。再次謝謝實驗室的各位學長姊弟妹，給我一個充實又快樂的碩班時光。

中文摘要



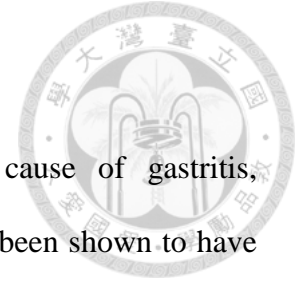
幽門桿菌為一種人類專一寄生的革蘭氏陰菌，於1982年由Warren和Marshall發現。幽門桿菌感染是造成胃炎、胃潰瘍、胃癌等疾病的一項重要因素，目前已有許多研究證明根除幽門桿菌可有效的預防胃癌。然而根除幽門桿菌療程冗長、藥物劑量高且會造成噁心、嘔吐等副作用，使得病人的順從性降低。此外臨床用於對抗幽門桿菌的抗生素包含阿莫西林、甲硝唑、四環素類等在胃酸環境下容易遭到破壞且難以滲入黏膜層，進而使根除率降低。

綜合上述問題，本實驗設計結合幾丁聚醣、聚丙烯酸以及磁性奈米粒子(Fe_3O_4)當作阿莫西林抗生素的載體。其中幾丁聚醣及聚丙烯酸皆具備黏膜貼附及良好的生物相容性的能力，已有大量文獻將其運用在口服藥物傳輸方便之研究，可有效延長載體在胃部滯留之時間，同時也可幫助載體滲入胃黏膜並接近幽門桿菌寄存之位置。再藉由外加磁場進一步使奈米載體快速貼附在黏膜，避免被胃部排出。聚丙烯酸會和阿莫西林競爭幾丁聚醣，因此當載體進入胃黏膜中藥物便會快速地釋放出來。

從藥物釋放測試及TEM觀察可以確定，我們設計的奈米載體可以在酸性環境下保持其結構完整且藥物不會持續釋放。而在中性環境下因幾丁聚醣變為電中性，使載體結構瓦解，阿莫西林便可迅速釋出。體外抑菌測試顯示載體可以良好的釋出阿莫西林展現良好的抑菌效果。

關鍵字:幽門桿菌、幾丁聚醣、聚丙烯酸、磁性奈米粒子

ABSTRACT



Helicobacter pylori (*H. pylori*) infection is the main cause of gastritis, gastroduodenal ulcers and gastric cancer. *H. pylori* eradication has been shown to have a prophylactic effect against gastric cancer. However, the long treatment time, large single dose of drug, and side effects of eradication therapy often lead to treatment failure.

In this study, the magnetic nanoparticles combined with chitosan and polyacrylic acid (PAA) is used as a drug nanoparticle for *H. pylori* eradication therapy. The muco-adhesive property of chitosan allows nanoparticles to adhere on the gastric mucosa. The location and residence time of nanoparticles could be controlled by the magnetic nanoparticles via magnetic field change. The addition of PAA could be used to compete with the drug for chitosan, so that drugs could be quickly released in the gastric mucosa for *H. pylori* eradication. Finally, the use of this nanoparticles could prolong the drug residence time in the stomach, reducing the drug dose and treatment time.

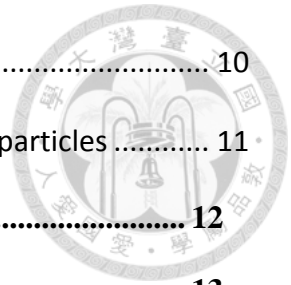
Keywords: *Helicobacter pylori*, nanoparticles, magnetic nanoparticle, chitosan, polyacrylic acid.

CONTENTS



論文口試委員會審定書	i
致謝	ii
中文摘要	iii
ABSTRACT	iv
CONTENTS	v
Chapter 1. Introduction	1
Chapter 2. Materials and Methods	4
2.1 Materials.....	4
2.2 Surface Functionalization of SPIO with APTES	4
2.3 Characterization of the SPIO@APTES Nanoparticles	4
2.4 Preparation of SPIO@PAA/CHI and SPIO/AMO@PAA/CHI Nanoparticles	4
2.5 Characterizations of SPIO@PAA/CHI and SPIO/AMO@PAA/CHI Nanoparticles	5
2.6 <i>In vitro</i> Drug Release.....	6
2.7 <i>In vitro</i> Bacterial Growth Inhibition.....	6
2.8 <i>In vitro</i> Mucoadhesive and Penetration	7
2.9 Development of Animal Model with <i>H. pylori</i> Infection	7
2.10 <i>In vivo</i> Anti- <i>H. pylori</i> Efficacy of SPIO/AMO@PAA/CHI Nanoparticles	8
Chapter 3. Result	9
3.1 Characterization of the SPIO@APTES Nanoparticles	9
3.2 Characterization of the SPIO/AMO@PAA/CHI Nanoparticles.....	9
3.3 <i>In vitro</i> Amoxicillin Release Profile	10
3.4 <i>In vitro</i> Bacterial Growth Inhibition.....	10

3.5 In vitro Mucoadhesive and Penetration.....	10
3.6 In vivo Anti-H. pylori Efficacy of SPIO/AMO@PAA/CHI Nanoparticles	11
Chapter 4. conclusion	12
REFERENCE	13
SCHEME.....	17
TABLE.....	18
FIGURE.....	20



LIST OF TABLE



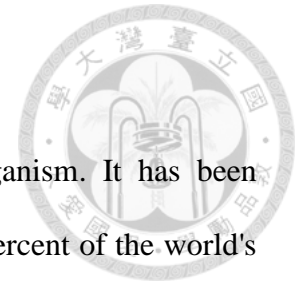
Table 1. APTES modify of SPIO	18
Table 2. Characterizations of nanoparticles	18
Table 3. In vivo anti- <i>H. pylori</i> efficacy.....	19

LIST OF FIGURES



Figure 1. APTES modify SPIO.....	20
Figure 2. FTIR test of SPIO with APTES modify	20
Figure 4. Effect of pH Variation on Particle Size, Zeta Potential and TEM	21
Figure 5 release profile of amoxicillin	22
Figure 6. In vitro bacterial growth inhibition.....	23
Figure 7. zeta potential of mucin.....	24
Figure 8. the mucopenetration of SPIO/AMO@PAA/CHI nanoparticle.....	25
Figure 9. PCR amplifications of <i>H. pylori</i> cagA gene.....	26

Chapter 1. Introduction



Helicobacter pylori (*H. pylori*) is a gram-negative microorganism. It has been proved by Warren and Marshall in 1982. There are more than 50 percent of the world's population infected by *H. pylori* ^[1]. The rate of infection even exceeds 80 percent of population in developing countries ^[2]. *H. pylori* is a prevalent human-specific pathogen which colonizes in stomach. It can penetrate through the gastric mucus layer to reach the epithelial cells underneath, and secreted urease to breaks down the urea present in the stomach to carbon dioxide and ammonia, which is used to neutralize gastric acid. *H. pylori* binds to gastric epithelial cells via various receptors, such as integrin $\beta 1$ (CD29) and fucosylated Lewis blood group antigens (Leb)^[3-6]. Furthermore, via HopQ, a paralog of the Hop family, binding to the carcinoembryonic antigen-related cell adhesion molecules (CEACAMs) on the gastric epithelial cells, *H. pylori* can enhance adhesion to host cell and subsequent translocation of cytotoxin-associated gene A (CagA) for virulence ^[7]. Above pathogenic mechanism will cause duodenal ulcers, gastric ulcers, and gastric adenocarcinoma in patients. Therefore, *H. pylori* has been considered an important factor that contributes to chronic inflammation of gastroduodenal, and listed in Group 1A carcinogens by International Agency for Research on Cancer (IARC) ^[8].

The triple therapy is a major clinical treatment regimen to eradicate *H. pylori* which was combine proton pump inhibitor (PPI) and two kinds of first line antibiotics including amoxicillin, metronidazole or clarithromycin. However, the triple therapy can't eradicate *H. pylori* completely due to several reasons. First, the activity of antibiotics will be destroyed by the gastric acid environment. Second, the concentration of antibiotic is difficult to get minimum inhibitory concentration (MIC) at *H. pylori* site

by the blood circulation. In addition; the antibiotics may cause patient dizziness, diarrhea and allergy that led to the patient with low drug compliance. Furthermore, with antimicrobial resistance strain increasing, the eradicated failure rate with triple therapy increases.

In order to solve above problems, we design a high-performance nanoparticle for *H. pylori* eradication, where chitosan is physically complexed with poly acrylic acid (PAA) and amoxicillin and super paramagnetic iron oxide (SPIO) to form nanoparticles (SPIO/AMO@PAA/CHI) with prolong the retention time in the stomach by the external magnetic field. Chitosan is the polymer of 2-amino-2-deoxy- β -d-glucan by glycosidic linkages. The primary amino groups of chitosan have special properties and make chitosan more useful in pharmaceutical applications. Chitosan has excellent biodegradable, non-toxic and mucoadhesive property. Chitosan has positive charges present in its chain that allow chitosan attract anionic polymers and drugs to produce many kinds of biomaterial products, including drug delivery system, wound dressing and antibacterial materials. Poly acrylic acid (PAA) is a synthetic polymer of acrylic acid. It is an anionic polymer, and has bioadhesion and biocompatibility. The degree of ionization of carboxyl groups was increase in the alkaline environment. PAA has been commonly used in the mucoadhesive delivery system. Amoxicillin could be protected in the designed nanoparticles in gastric acid environment (pH=1.2), and released in the *H. pylori* site (pH=7.4) where the environmental pH is higher than the pKa value of chitosan, the surface charge of chitosan would be lost, and particle structure would disintegrate.

SPIO is a popular metal material, among them, the Fe₃O₄ with inverse spinel structure has high magnetic. The common methods of preparation of Fe₃O₄ include grinding, thermal cracking and chemical co-precipitation^[9-10]. The thermal cracking

methods has advantage of average particle size but it need to use oleic acid as protective agent and crack iron into Fe_3O_4 nanoparticles in the high temperature. SPIO has been applied for the target lesion, drug release systems, contrast media, hypothermia treatment and Gene transfer ^[11-14].

The developed SPIO/AMO@PAA/CHI nanoparticles were characterized using the Zetasizer and transmission electron microscope (TEM). The loading efficiency of amoxicillin in SPIO/AMO@PAA/CHI was measured by High-performance liquid chromatography. And SPIO/AMO@PAA/CHI was cultured with *H. pylori* to evaluate whether it could inhibit the growth of *H. pylori*. Furthermore, the biodistribution of SPIO/AMO@PAA/CHI and *H. pylori* eradication efficiency were determined *in vivo* after exposure to magnetic fields.

Chapter 2. Materials and Methods



2.1 Materials

SPIO were kindly supplied by Gene'e Tech Co., Ltd. (Taiwan). PAA (M.W. 100 kDa, 35 wt%), amoxicillin, and 3-Aminopropyltriethoxysilane (99%) from Sigma-Aldrich (USA). Chitosan was purchased from Polysciences, Inc (USA). Mucin from porcine stomach were purchased from Sigma-Aldrich (USA).

2.2 Surface Functionalization of SPIO with APTES

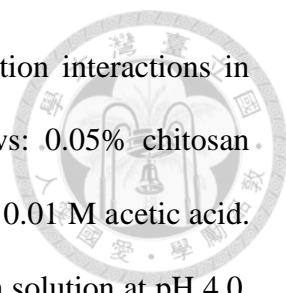
In a glass container under ambient conditions, 1 μ l of 3-aminopropyltriethoxysilane solution was added to a dispersion of hydrophobic SPIO nanoparticles in hexane (2 mg in 30 mL) containing 0.01% (v/v) acetic acid. The mixture was shaken violently for 72 h, during which the particles precipitated and attached on the bottle wall. The particles were washed three times with hexane to remove all excess silanes and dried at the room temperature.

2.3 Characterization of the SPIO@APTES Nanoparticles

The chemical compositions of SPIO and SPIO@APTES were characterized with an ATR-FTIR spectrometer (Thermo Scientific Nicolet 6700; MA, USA) to determine the characteristics of the SPIO and SPIO@APTES nanoparticles. Superconducting Quantum Interference Device Magnetometer (SQUID, MPMS3; USA) was used to determine the magnetic characteristics of the prepared SPIO@APTES nanoparticles. Magnetization curves as a function of magnetic field were measured at 300 K for magnetic fields up to 3.0 Tesla.

2.4 Preparation of SPIO@PAA/CHI and SPIO/AMO@PAA/CHI Nanoparticles

The preparation of nano-particles loaded with amoxicillin and SPIO was based on the ionic gelation interaction ^[15]. Ionized amoxicillin and SPIO with negative and



positive charge, respectively, also partially contributed to the gelation interactions in this study. The preparation process is briefly described as follows: 0.05% chitosan solution was prepared by dissolving 0.5 mg chitosan powder in 1 ml 0.01 M acetic acid. Then 1 mg of SPIO powder was dissolved in 5 ml of 0.05% chitosan solution at pH 4.0. 0.15% amoxicillin solution was prepared by dissolving 1.5 mg 5-ALA powder in 1 ml 0.015% or 0.02 % PAA solution, where PAA were dissolved in 0.01 M NaOH solution beforehand. Two milliliter of PAA solution or 2 ml of amoxicillin solution with pH value of 7.4 were added to 5 ml of chitosan/SPIO solution with a peristaltic pump at a flow rate of 0.5 ml/min to prepare the SPIO@PAA/CHI and SPIO/AMO@PAA/CHI nanoparticles. The prepared SPIO@PAA/CHI and SPIO/AMO@PAA/CHI suspended in the solution were later used directly without further treatment.

2.5 Characterizations of SPIO@PAA/CHI and SPIO/AMO@PAA/CHI Nanoparticles

The particle size and zeta-potential of the prepared nanoparticles were determined by using a Zetasizer Nano-ZS90 (Malvern Instruments, Worcestershire, UK) based on dynamic light scattering measurements and laser Doppler electrophoresis, respectively. Particle size was measured at 25 °C with a 90° scattering angle based on the Zetasizer Nano-ZS90 internal setting. The cumulative curve was used to present the mean hydrodynamic diameter. Measurements of zeta-potentials were made using the aqueous flow cell in the automatic mode at 25 °C.

In order to determine the morphology of the SPIO/AMO@PAA/CHI nanoparticles at different pHs, carbon-coated 200-mesh copper grids were immersed in SPIO/AMO@PAA/CHI solutions at pH 2.5, 4.0, 5.0, 6.5, and 7.4. Grids were placed on delicate-task-wipes to absorb excess liquid and then dried in a desiccator overnight. The dried copper grids with SPIO/AMO@PAA/CHI were examined under a transmission

electron microscopy (TEM, Hitachi H-7500, Tokyo, Japan).

The loading efficiency of amoxicillin in the prepared nanoparticle was determined by using the high-performance liquid chromatography (HPLC, Waters e2696). Briefly, after preparation of SPIO/AMO@PAA/CHI nanoparticles and centrifugation at 16,000 g for 10 min, the supernatant was passed through a 0.22- μ m filter, and 10 μ L of the filtered supernatant was injected into the HPLC system. Separation was achieved on a Waters Symmetry-C18 reversed-phase column (XBridgeTM). The mobile phase consisted of 5% acetonitrile at a flow rate of 1 mL/min. The unloaded amoxicillin was detected by UV detector at a wavelength of 229 nm. The drug loading efficiency (L.E.) was calculated by using the following equation:

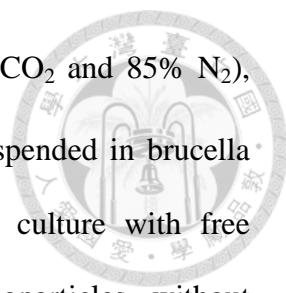
Loading efficiency (%) = (Weight of the feeding amoxicillin – Weight of the unloaded amoxicillin)/ Weight of the feeding amoxicillin \times 100%

2.6 *In vitro* Drug Release

The drug-release profiles of amoxicillin from SPIO/AMO@PAA/CHI nanoparticles were analyzed by using the dialysis-bag diffusion method ^[16]. Briefly, a total of 10 ml of the prepared nanoparticle solution were concentrated using Amicon Ultra centrifugal filter devices (Millipore, Billerica, MA, USA) to remove the unloaded amoxicillin, then loaded in a CelluSep dialysis membrane (Membrane Filtration Products, Seguin, TX, USA), which had a molecular weight cut-off of 3.5 kD. The dialysis membrane was soaked in 45 ml of buffer at pH 2.5 for 2 h, pH 6.5 for 2 h, and then pH 7.4 for 48h at 37 °C to simulate the pH value in the stomach environments, respectively. After shaking at 100 rpm for a period of time, 1 ml of the buffer was removed, and the optical density (OD) of amoxicillin was recorded by HPLC.

2.7 *In vitro* Bacterial Growth Inhibition

Seven *H. pylori* strains with different MIC were culture on the blood agar plates at



37°C for 3 days under a microaerophilic condition (5% O₂, 10% CO₂ and 85% N₂), respectively. Then *H. pylori* were harvested from plates and re-suspended in brucella broth (Sigma-Aldrich, USA) with 10% fetal bovine serum and culture with free amoxicillin, SPIO@PAA/CHI and SPIO/AMO@PAA/CHI nanoparticles without amoxicillin and nanoparticles for 48 hours. Finally, the OD of brucella broths containing *H. pylori* were determined by ultraviolet–visible (UV–Vis) spectrophotometer (Cary 50 Conc; Varian, Palo Alto, CA, USA) at 600nm

2.8 In vitro Mucoadhesive and Penetration

The mucoadhesive test was determined by zeta potential.^[17] The various volume mucin with 1mg/ml concentration and mix PAA or chitosan with concentration 0.5mg/ml at pH 4.5.

The FITC-chitosan was used to penetration test. The 300µl mucin in 48 well and SPIO@PAA/CHI particles were loaded onto mucin slowly. All sample were shake 80rpm, 15min with magnetic field or nonmagnetic field. Then the sample was freeze at -80° C and embed with optimal cutting temperature compound (OCT). Slice sample by frozen section and observed by fluorophores.

2.9 Development of Animal Model with *H. pylori* Infection

The pathogen-free BALB/c mice with 4 weeks age were purchased from the National Laboratory Animal Center (Taipei, Taiwan). The *in vivo* experimental protocols were approved by the National Taiwan University College of Medicine and College of Public Health Institutional Animal Care and Use Committee.^[18] To induce *H. pylori* infection, each BALB/c mouse was fed with 0.2 ml of 2×10⁸ CFU/ml *H. pylori* in the BHI broth twice a day for two consecutive days, and then the infection was allowed to develop for two weeks.

2.10 In vivo Anti-*H. pylori* Efficacy of SPIO/AMO@PAA/CHI Nanoparticles

All infected mouse were randomly divided 4 group (n=6) and orally administrated with PBS, free amoxicillin solution, SPIO/AMO@PAA/CHI nanoparticles and SPIO/AMO@PAA/CHI nanoparticles with magnetic field treatment for 1 hour. Administration was performed once a day for five consecutive days. Twenty-four hours after last administration, mice were sacrificed and stomachs were collected. The half stomach tissue were rinsed with PBS. Then sample with few BHI broth was grinded by the mortar and pestle to the broth. Then the sample broth was added on the select agar plates and cultured at 37°C under a microaerophilic condition for 2 days. Then bacterial colonies were harvested by a sterile cotton swab and resuspended in PBS. In order to confirm *H. pylori* status, the bacterial resuspended solutions were adapted by polymerase chain reaction (PCR) to determine the CagA-gene expression ^[19,20]. The other half of stomach was fixed in 10% formalin and embedded in paraffin wax for histological assessment.

Chapter 3. Result



3.1 Characterization of the SPIO@APTES Nanoparticles

The SPIO nanoparticles fabricated via thermal decomposition method were supplied by Gene'e Tech Co., Ltd. The SPIO nanoparticles were surface functionalized with APTES to possess amino groups on the particle surface (Figure 1). As shown in Table 1, When the SPIO nanoparticles were modified with APTES, the particle size and zeta potential increased from 16.9 nm to 40.0 nm and 32.1 mV to 52 mV, respectively. The higher the zeta potential, the more positive charges of amino groups are present on the nanoparticles' surface. Along with increase the amount of APTES added, the particle size of SPIO@APTES increased, but zeta potential hadn't significant change. Thus, we chose 1 μ l of APTES as a best SPIO modification condition for subsequent experiments.

The FT-IR spectra of the SPIO and SPIO@APTES were shown in Figure 2. Characteristic FT-IR absorption peaks at 2850 and 2920 cm^{-1} observed in the spectrum of SPIO were assigned to the asymmetric and symmetric $-\text{CH}_2$ stretching bands ^[21], which were presented in the structure of oleic acid as capping molecules. The absorption bands at 1720 cm^{-1} was attributed to the asymmetric stretching vibrations of the COO^- groups of oleic acid ^[22]. When the capping molecules, oleic acid, on SPIO nanoparticles were ligand-exchanged with APTES, two new absorption peaks at 1100 cm^{-1} (symmetric stretching Si–O–Si bonds) and 1529 cm^{-1} (N-H bending of primary amines) appeared in the FT-IR spectrum of SPIO@APTES ^[23].

3.2 Characterization of the SPIO/AMO@PAA/CHI Nanoparticles

The particle size and zeta potential of chi/PAA nanoparticles was show in Table 2. We try several concentrations of PAA 0.1, 0.15, 0.2 and 0.25 mg/ml to synthesis

nanoparticles. Because PAA has anion charge, the drug loading efficiency was better in high PAA concentration but the particle size with rise. The 0.15 and 0.2 concentration of PAA was choosing to subsequent experiment.

The effect of pH variation on chi/PAA nanoparticle size, zeta-potential and shape was show in figure 3. Chi/PAA nanoparticle can maintain shape and size at pH value below 6.5. Chitosan was Electrical neutral at pH 7.4, the particle was collapse and aggregation.

3.3 In vitro Amoxicillin Release Profile

As show in figure 5, amoxicillin was keeping in the particles at pH 2.5 and pH6.5. When the particle collapsed, amoxicillin was release fast at pH 7.4. At 48 hours, the release rate of amoxicillin from 0.2PAA nanoparticle was higher than that from 0.15PAA nanoparticle, indicating that more PAA incorporation could reduce the intensity of the interaction between chitosan and amoxicillin by competing for cationic residues, thereby allowing release of amoxicillin under these conditions.

3.4 In vitro Bacterial Growth Inhibition

Figure 6 show the bacterial growth inhibition. We choose several *H. pylori* strains which minimum inhibitory concentration (MIC) of amoxicillin is between 0.5ug/ml to 0.016ug/ml. The antibacterial ability of chitosan has been proved thus the treatment approach with nanoparticle without amoxicillin has slightly inhibited. Our nanoparticle shows the same bacterial growth inhibition ability as amoxicillin solution that indicated amoxicillin of nanoparticle was release completely.

3.5 In vitro Mucoadhesive and Penetration

The mucoadhesive was show in the figure 7. Chitosan has been known that has mucoadhesive ability. In the figure 7(B), the zeta potential of chitosan and mucin was increased as concentration increased. Zeta potential was approach pure chitosan at high concentration. In the figure 7(C), SIPO@APTES hasn't mucoadhesive property which

zeta potential hasn't significant change. In the figure 7(A), SPIO@PAA/CHI and SPIO/AMO@PAA/CHI nanoparticle show the similar variety with figure 7(B). It proved that our nanoparticle has mucoadhesive property.

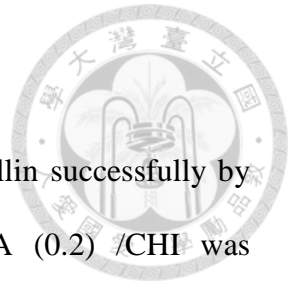
Figure 8 show the mucopenetration of SPIO/AMO@PAA/CHI nanoparticle. The nanoparticle with magnetic fields has significant signal at bottom of mucin. It is show that SPIO with magnetic fields can assist nanoparticle penetrate mucin get to *H. pylori* site.

3.6 In vivo Anti-*H. pylori* Efficacy of SPIO/AMO@PAA/CHI Nanoparticles

Table 3 show the in vivo eradication rate of *H. pylori*. In the in vivo study, the eradication rate of PBS group is 0%. Because without PPI, only a mice has been heal in the amoxicillin solution group. Compare SPIO/AMO@PAA/CHI nanoparticle with magnetic fields and without magnetic fields. The SPIO/AMO@PAA/CHI nanoparticle without magnetic fields shows the better eradication rate than SPIO/AMO@PAA/CHI nanoparticle with magnetic fields. It probably because we used magnetic fields is single direction which cause lots of nanoparticle focus on one side. The nanoparticle can't distribute to whole stomach led to the eradication rate decreased.

Chapter 4. conclusion


In this study, we combined chitosan, PAA, SPIO and amoxicillin successfully by ionic gelation method. The particles size of SPIO/AMO@PAA (0.2) /CHI was 167.3 ± 4.57 nm and drug loading efficiency reach up to 77.8 ± 0.63 %. Morphology of the SPIO/AMO@PAA/CHI nanoparticles at different pH value shows that our nanoparticle has pH-sensitive property. It can maintain shape and protect amoxicillin at acid environment and collapse at pH 7.4. The Release profile test proved that SPIO/AMO@PAA/CHI nanoparticles can keep amoxicillin inside until Neutral environment. The release of amoxicillin was higher than 90% at 48 hours. In vitro bacterial growth inhibit show that the antibacterial ability of SPIO/AMO@PAA/CHI nanoparticles as same as free amoxicillin solution. In mucoadhesive and mucopenetration study show that the SPIO/AMO@PAA/CHI nanoparticles has ability to adhere and penetrate mucous. In the in vivo study, our nanoparticles has 50% eradication rate without PPI. Single direction magnetic fields led to eradication rate decrease. Switch to ring magnetic fields may improve the distribution of nanoparticle.




REFERENCE



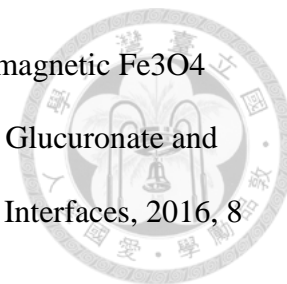
- [1] Pounder RE, Ng D. The prevalence of *Helicobacter pylori* infection in different countries. *Aliment Pharmacol Ther* 1995; 9(Suppl 2): 33-9.
- [2] Torres J, Leal-Herrera Y, Perez-Perez G, et al. A communitybased seroepidemiologic study of *Helicobacter pylori* infection in Mexico. *J Infect Dis* 1998; 178: 1089-94.
- [3] B. Kaplan-Turkoz, L. F. Jimenez-Soto, C. Dian, C. Ertl, H. Remaut, A. Louche, T. Tosi, R. Haas, L. Terradot, Structural insights into *Helicobacter pylori* oncoprotein CagA interaction with $\beta 1$ integrin *Proc. Natl. Acad. Sci. U.S.A.* 2012, 109, 14640.
- [4] T. Koelblen, C. Berge, M. V. Cherrier, K. Brillet, L. Jimenez-Soto, L. Ballut, J. Takagi, R. Montserret, P. Rousselle, W. Fischer, R. Haas, R. Fronzes, L. Terradot. Molecular dissection of protein-protein interactions between integrin $\alpha 5 \beta 1$ and the *Helicobacter pylori* Cag type IV secretion system. *FEBS J.* 2017, 284, 4143.
- [5] Y. Y. Fei, A. Schmidt, G. Bylund, D. X. Johansson, S. Henriksson, C. Lebrilla, J. V. Solnick, T. Boren, X. D. Zhu, Use of Real-Time, Label-Free Analysis in Revealing Low-Affinity Binding to Blood Group Antigens by *Helicobacter pylori*. *Anal. Chem.* 2011, 83, 6336.
- [6] P. Parreira, Q. Shi, A. Magalhaes, C. A. Reis, J. Bugaytsova, T. Boren, D. Leckband, M. C. L. Martins. Atomic force microscopy measurements reveal multiple bonds between *Helicobacter pylori* blood group antigen binding adhesin and Lewis b ligand. *J. R. Soc. Interface* 2014, 11, articlenumber 20141040.
- [7] V. Koniger, L. Holsten, U. Harrison, B. Busch, E. Loell, Q. Zhao, D.A. Bonsor, A. Roth, A. Kengmo-Tchoupa, S. I. Smith, S. Mueller, E. J. Sundberg, W. Zimmermann, W. Fischer, C. R. Hauck, R. Haas, *Helicobacter pylori* exploits

- 
- human CEACAMs via HopQ for adherence and translocation of CagA.
Nat.Microbiol. 2016, 2, article number 16188.
- [8] Park S, Kim WS, Choi UJ, Han SU, Kim YS, Kim YB, et al. Amelioration of oxidative stress with ensuing inflammation contributes to chemoprevention of H.pylori-associated gastric carcinogenesis. *Antioxid Redox Signal* 2004; 6: 549-560.
- [9] N. Shamim, L. Hong, K. Hidajat, M.S.(2007) Uddin. Thermosensitive polymer (*N*-isopropylacrylamide) coated nanomagnetic particles: Preparation and characterization. *Colloids and Surfaces B: Biointerfaces* 55, 51–58.
- [10] A.G. de Boer and P.J. Gaillard. Drug Targeting to the Brain. *Annu. Rev. Pharmacol. Toxicol.* 2007;47:323–355.
- [11] Suzuki M, M. Shinkai, M. Yanase, A. Ito, H. Honda and T. and Kobayashi. Enhancement of uptake of magnetoliposomes by magnetic force and hyperthermic effect on tumor. *Jpn J HyperthermicOncol* 15(1999):79-87.
- [12] Shinkai M. (2002)Functional magnetic particles for medical application. *J Biosci Bioeng.*;94(6):606-13.
- [13] Huh YM, Jun YW, Song HT, Kim S, Choi JS, Lee JH, Yoon S, Kim KS, Shin JS, Suh JS and Cheon J(2005) In vivo magnetic resonance detection of cancer by using multifunctional magnetic nanocrystals. *J Am ChemSoc* 127:12387-12391.
- [14] Jian Lu, Shuli Ma, Jiayu Sun, Chunchao Xia, Chen Liu, Zhiyong Wang, Xuna Zhao, Fabao Gao, Qiyong Gong, Bin Song, Xintao Shuai, Hua Ai, and Zhongwei Gu.(2009)Manganese ferrite nanoparticle micellarnanocomposites as MRI contrast agent for liver imaging. *Biomaterials.* 30: 2919–2928.
- [15] Yang SJ, Lin FH, Tsai HM, Lin CF, Chin HC, Wong JM, Shieh MJ Alginate-folic acid-modified chitosan nanoparticles for photodynamic detection of intestinal

neoplasms, *Biomaterials*. 2011 Mar;32(8):2174-82.

- 
- [16] Cheng-Liang Peng, Li-Yuan Yang, Tsai-Yueh Luo, Ping-Shan Lai, Shu-Jyuan Yang, Wu-Jyh Lin and Ming-Jium Shieh. Development of pH sensitive 2-(diisopropylamino)ethyl methacrylate based nanoparticles for photodynamic therapy. *Nanotechnology* 21 (2010) 155103.
- [17] Hirofumi Takeuchi, Jringjai Thongborisute, Yuji Matsui, Hikaru Sugihara, Hiromitsu Yamamoto, Yoshiaki Kawashima. Novel mucoadhesion tests for polymers and polymer-coated particles to design optimal mucoadhesive drug delivery systems. *Advanced Drug Delivery Reviews* 57 (2005) 1583– 1594
- [18] Yang JC, Wang TH, Wang HJ, Kuo CH, Wang JT, Wang WC. Genetic analysis of the cytotoxin-associated gene and the vacuolating toxin gene in *Helicobacter pylori* strains isolated from Taiwanese patients. *Am J Gastroenterol*. 1997; 92:1316-21.
- [19] Jyh-Chin Yang, Chia-Tung Shun, Chiang-Ting Chien, and Teh-Hong Wang. Effective Prevention and Treatment of *Helicobacter pylori* Infection Using a Combination of Catechins and Sialic Acid in AGS Cells and BALB/c Mice, *J.Nutr*. 2008, 138: 2084–2090.
- [20] Wang JT, Lin JT, Sheu JC, Yang JC, Chen DS, Wang TH. Detection of *Helicobacter pylori* in gastric biopsy tissue by polymerase chain reaction. *Eur J Clin Microbiol Infect Dis*. 1993;12:367-71.
- [21] Randy De Palma, Sara Peeters, Margriet J. Van Bael, Heidi Van den Rul, Kristien Bonroy, Wim Laureyn, Jules Mullens, Gustaaf Borghs, and Guido Maes. Silane Ligand Exchange to Make Hydrophobic Superparamagnetic Nanoparticles Water-Dispersible *Chem. Mater.*, 2007, 19 (7), pp 1821–1831
- [22] Patsula V, Kosinová L, Lovrić M, Ferhatovic Hamzić L, Rabyk M, Konefal R,

Paruzel A, Šlouf M, Herynek V, Gajović S, Horák D. Superparamagnetic Fe₃O₄ Nanoparticles: Synthesis by Thermal Decomposition of Iron(III) Glucuronate and Application in Magnetic Resonance Imaging. ACS Appl. Mater. Interfaces, 2016, 8 (11), pp 7238–7247

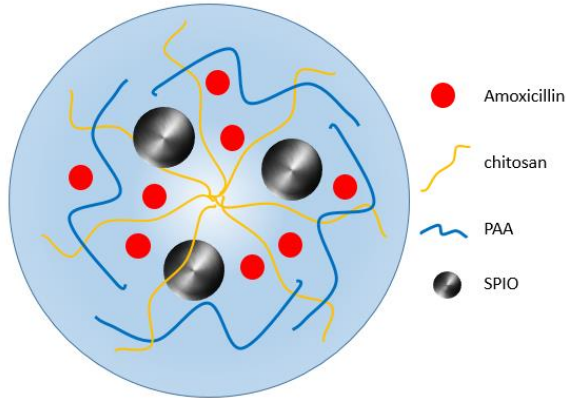


[23] Manuel Cano, Rebeca Núñez-Lozano, Yves Dumont, Chantal Larpent and Guillermo de la Cueva-Méndez Synthesis and characterization of multifunctional superparamagnetic iron oxide nanoparticles (SPION)/C60 nanocomposites assembled by fullerene–amine click chemistry RSC Adv., 2016,6, 70374-70382

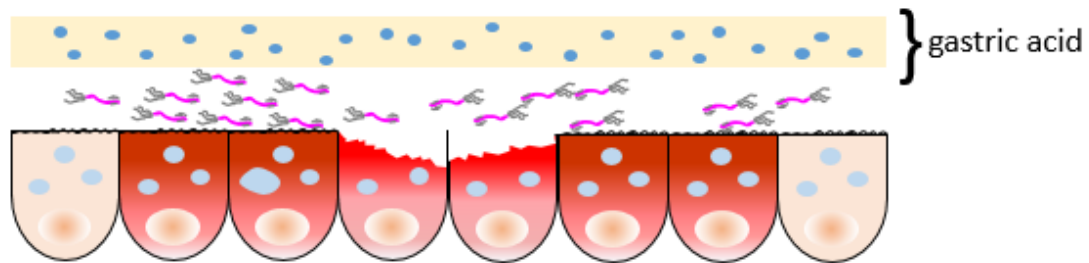
SCHEME



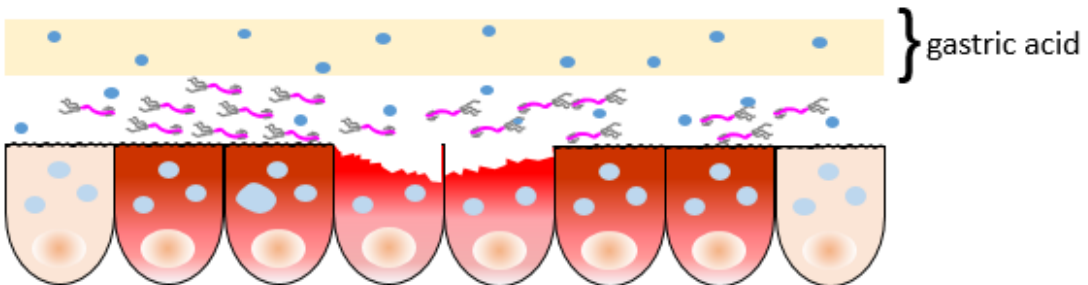
(A)



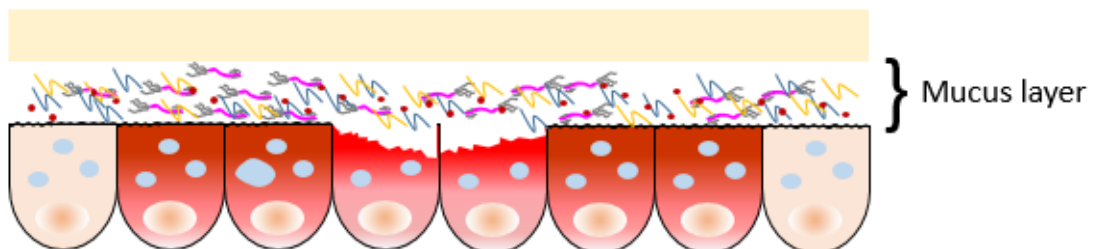
(B)



(C)



(D)



(A) SPIO/AMO@PAA/CHI nanoparticles, (B) nanoparticles were stable in gastric acid, (C) nanoparticles adhere and infiltrate into the mucus layer of gastric tract, (D) the infiltrate nanoparticles contract with *H. pylori* of gastric epithelium or tight junction, then its becoming unstable may release drug at the site of *H. pylori*

TABLE



Table 1. APTES modify of SPIO

	APTES content (ml)	SIZE (nm)	PDI	Zeta Potential (mV)
Fe ₃ O ₄		16.92	0.141	32.1 ± 0.92
Fe ₃ O ₄ @APTES	1	41.0 ± 1.40	0.276	52.0 ± 0.62
Fe ₃ O ₄ @APTES	2	47.2 ± 2.69	0.263	51.4 ± 0.72
Fe ₃ O ₄ @APTES	4	46.5 ± 2.39	0.272	49.0 ± 0.63
Fe ₃ O ₄ @APTES	6	49.5 ± 4.64	0.235	50.1 ± 0.13

Table 2. Characterizations of nanoparticles

	Average size (nm)	PDI	Zeta potential (mV)	Loading efficiency (%)
SPIO@PAA(0.1)/CHI	126.8±7.29	0.507	46.7±1.72	—
SPIO/AMO@PAA(0.1) CHI	139.5±2.50	0.488	45.0±0.96	72.7±0.10
SPIO@PAA(0.15)/CHI	142.4±2.33	0.386	48.0±0.99	—
SPIO/AMO@PAA(0.15)/CHI	151.9±7.92	0.375	45.9±1.22	75.5±0.44
SPIO@PAA(0.2)/CHI	150.4±1.64	0.338	48.2±1.45	—
SPIO/AMO@PAA(0.2)/CHI	167.3±4.57	0.303	46.5±1.05	77.8±0.63
SPIO@PAA(0.25)/CHI	177.6±5.54	0.300	48.5±1.71	—
SPIO/AMO@PAA(0.25)/CHI	189.0±1.83	0.320	46.3±0.65	78.8±1.61
SPIO@PAA(0.3)/CHI	187.7±7.36	0.320	48.1±1.18	—
SPIO/AMO@PAA(0.3)/CHI	201.8±7.57	0.337	47.5±0.68	79.1±0.09

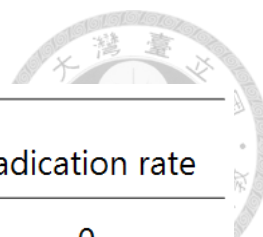


Table 3. In vivo anti-*H. pylori* efficacy

GRUOP	1	2	3	4	5	6	Eradication rate
PBS solution	+	+	+	+	+	+	0
Amoxicillin solution	+	+	+	-	+	+	16.67%
SPIO/AMO@PAA/CHI nanoparticle	-	+	+	+	-	-	50%
SPIO/AMO@PAA/CHI nanoparticle + magnetic fields (1 hour)	+	+	+	-	+	+	16.67%

FIGURE

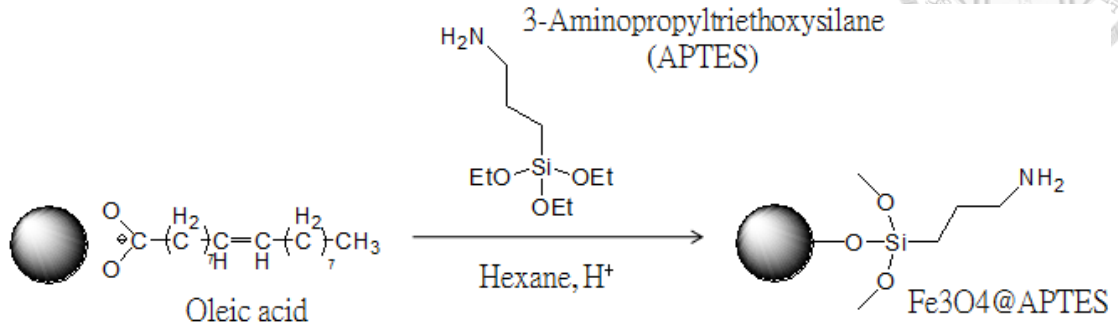


Figure 1. APTES modify SPIO

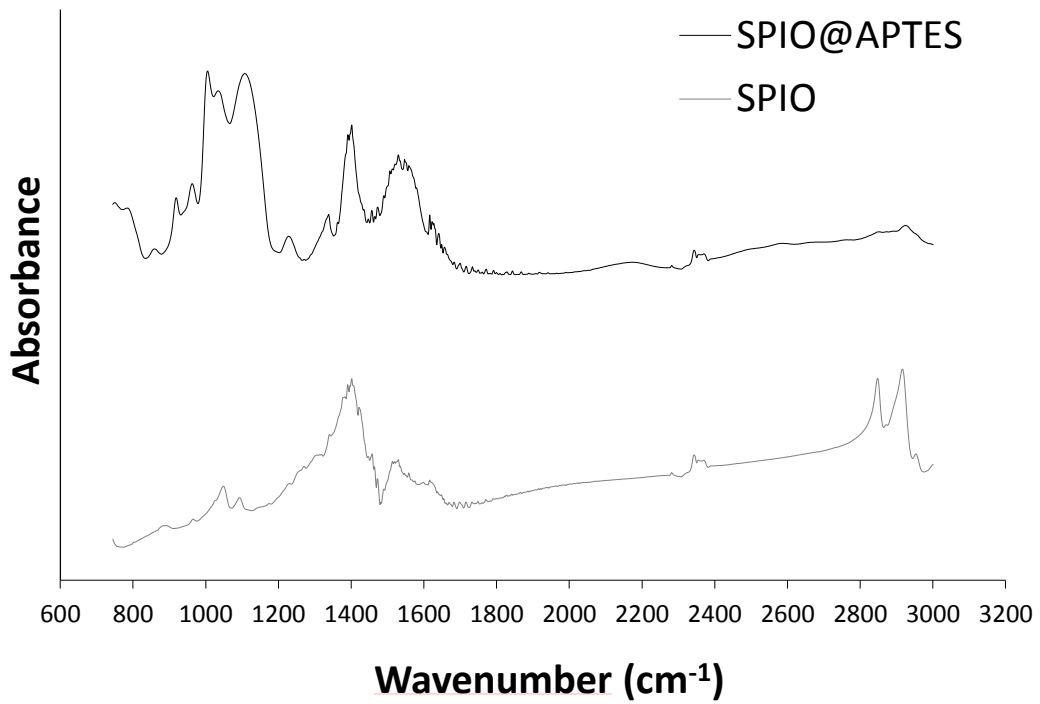
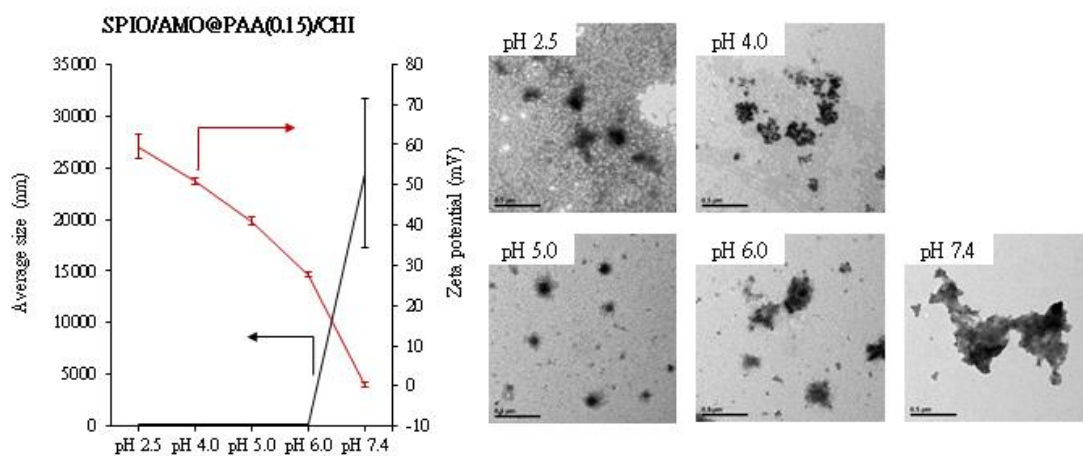


Figure 2. FTIR test of SPIO with APTES modify



(A)



(B)

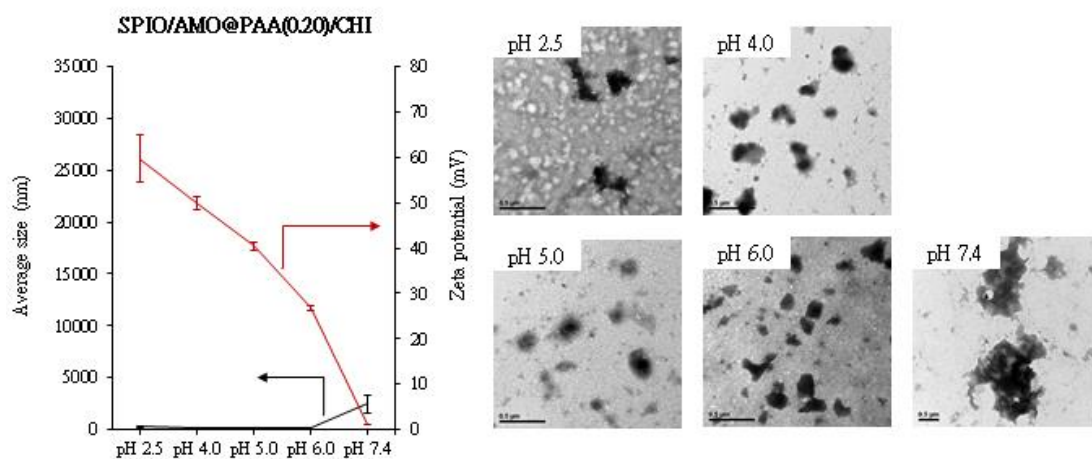


Figure 4. Effect of pH Variation on Particle Size, Zeta Potential and TEM (A) 0.15PAA (B) 0.2PAA

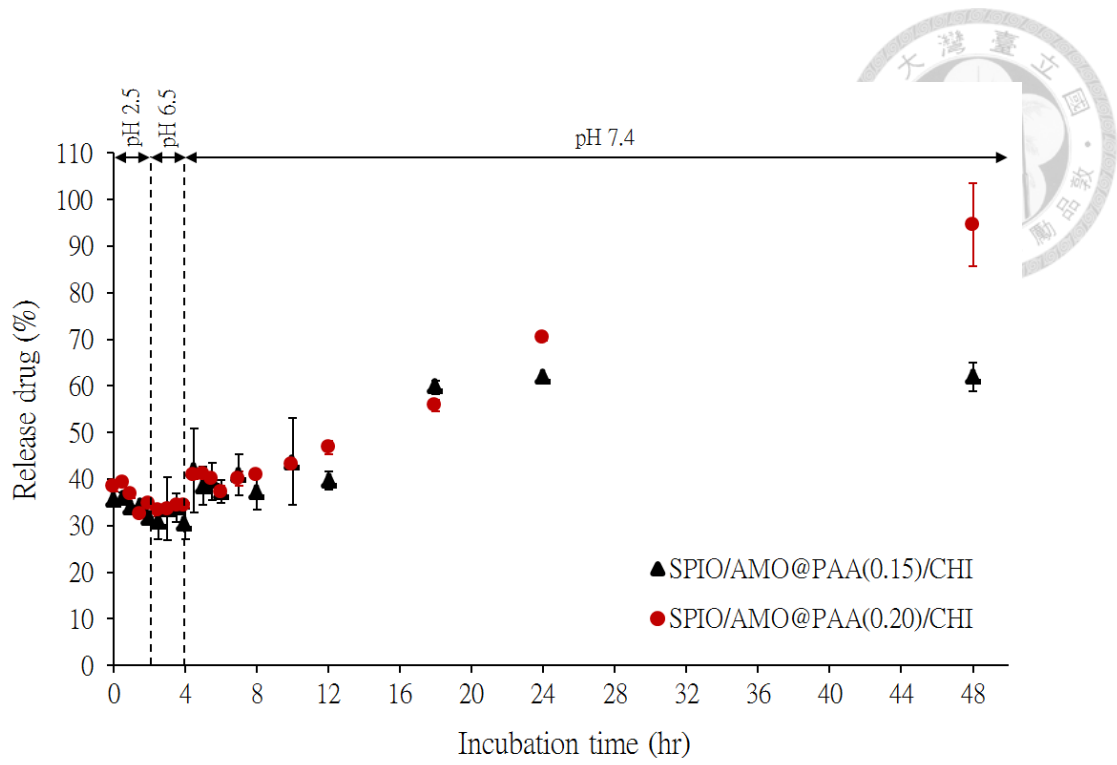


Figure 5 release profile of amoxicillin

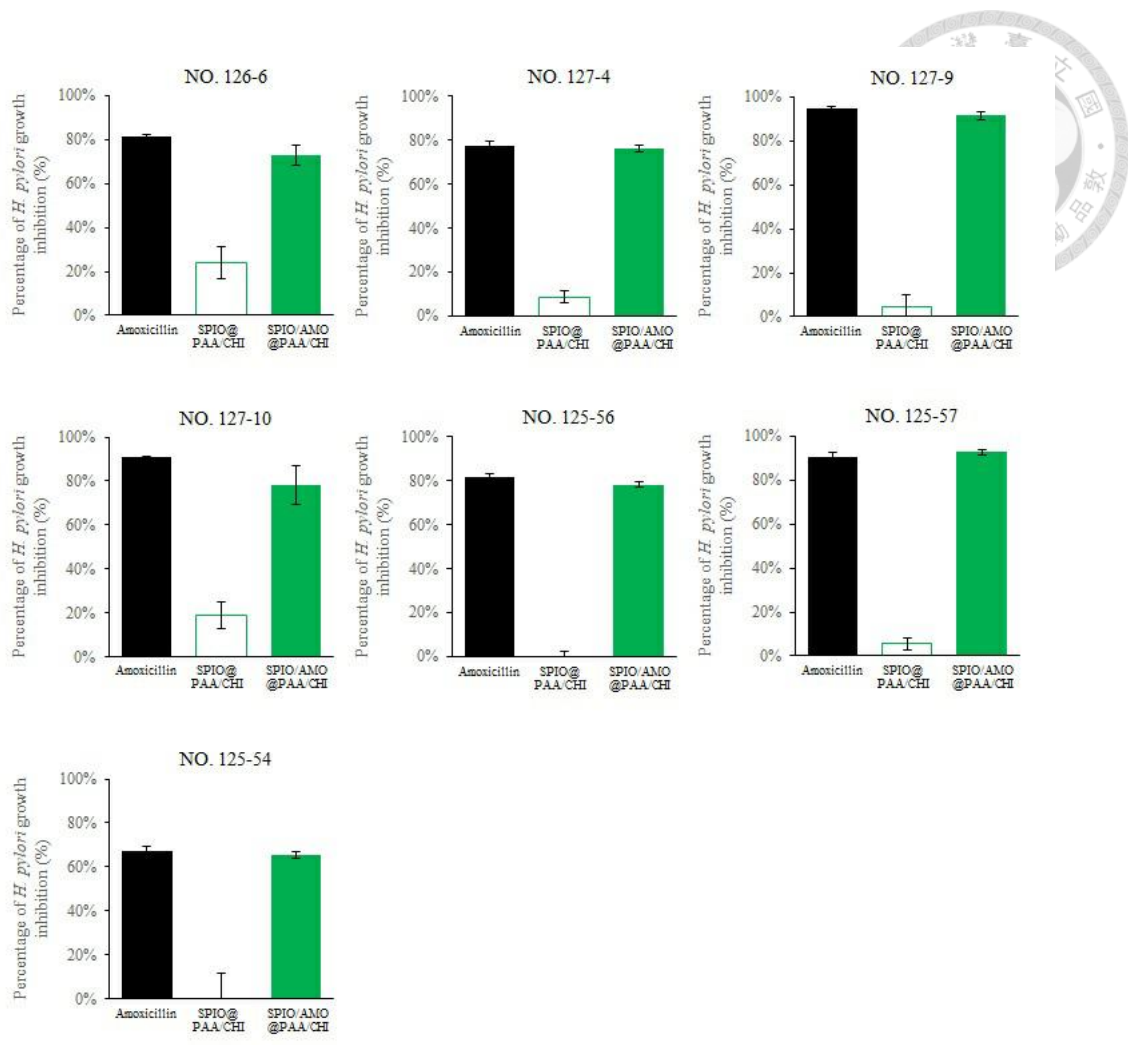


Figure 6. In vitro bacterial growth inhibition, the MIC of amoxicillin is between 0.5ug/ml to 0.016ug/ml

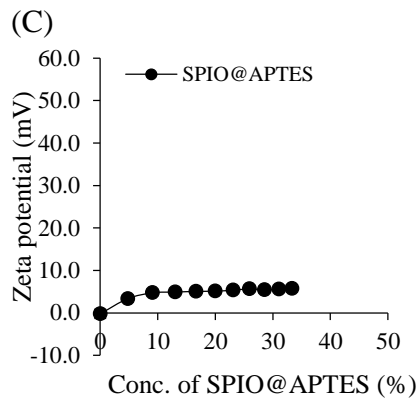
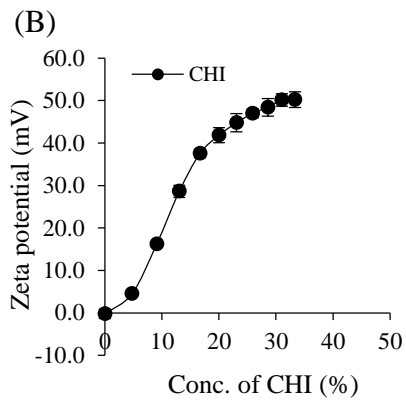
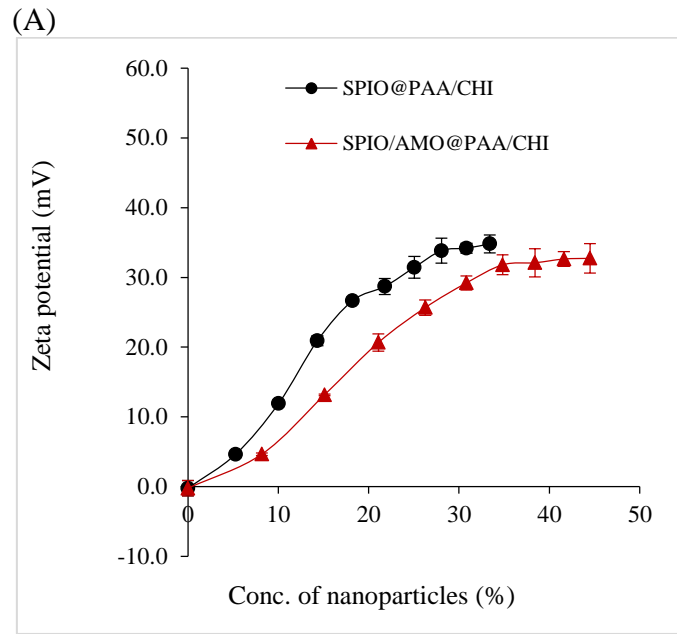
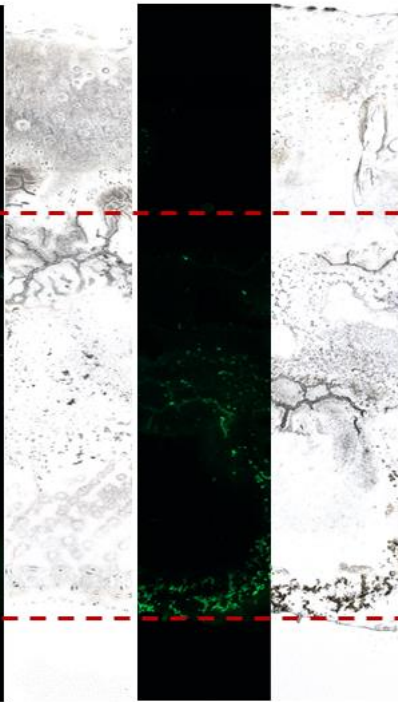
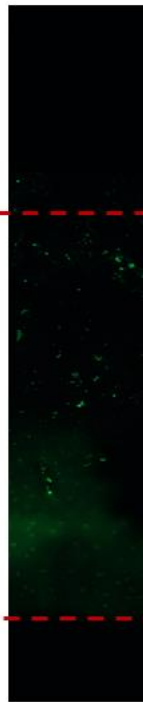


Figure 7. zeta potential of mucin with (A) SPIO@PAA/CHI and SPIO/AMO@PAA/CHI (B) chitosan (C) SPIO@APTES

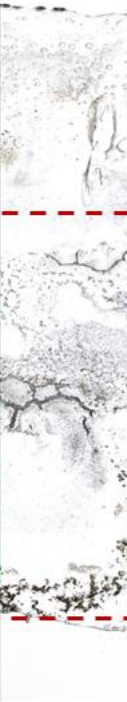
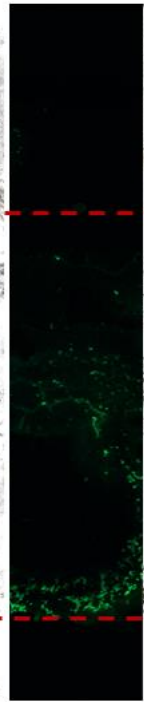
SPIO/AMO@PAA/C
HI nanoparticle

15 min

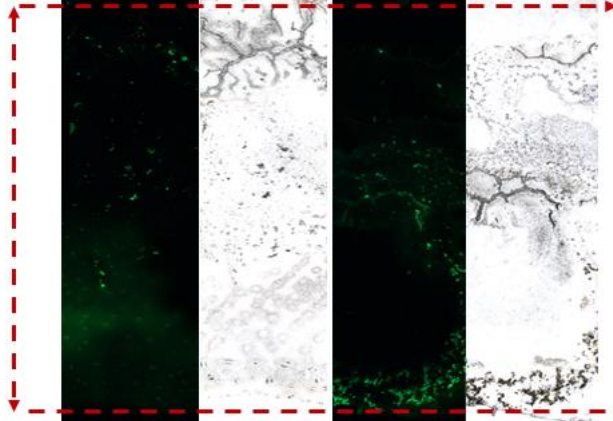


SPIO/AMO@PAA/CHI
nanoparticle + magnetic fields

15 min



1700 μ l



Bottom of mucin

Figure 8. the mucopenetration of SPIO/AMO@PAA/CHI nanoparticle

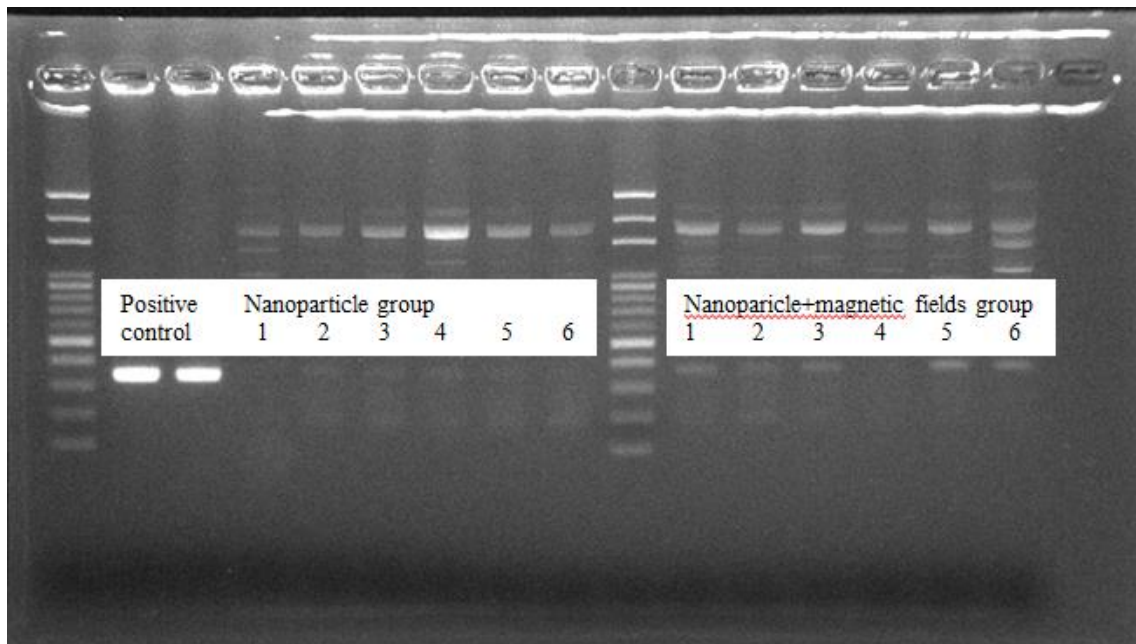
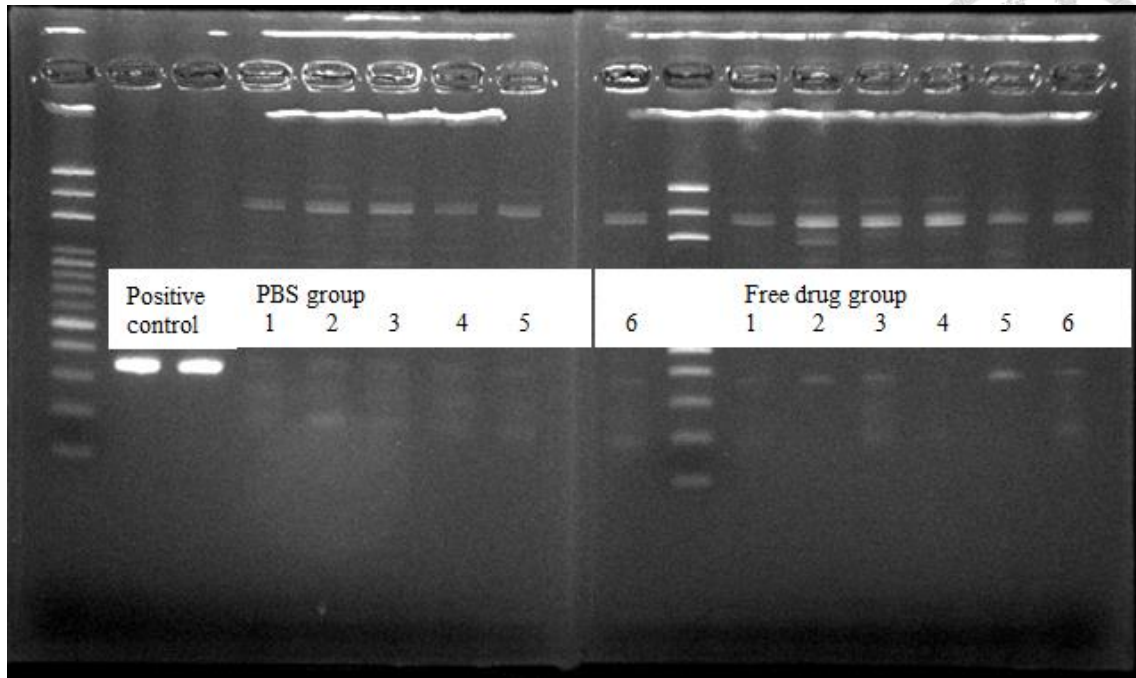


Figure 9. PCR amplifications of *H. pylori* cagA gene